

# Optical Anisotropy of Carbon Nitride Thin Films and Photografted Polystyrene Brushes

Paolo Giusto,\* Baris Kumru,\* Daniel Cruz, and Markus Antonietti

Polymer brushes on surfaces enable advanced material design. In the present contribution, transparent and flat photoactive polymeric carbon nitride (pCN) thin films are employed as a photoactive substrate and primer layer to grow polystyrene (PS) brushes. These films are then characterized by ellipsometry. For the first time herein is reported on the optical anisotropy of pCN thin films revealing a high positive birefringence up to 0.71 with an in-plane  $n_D$  of 2.54 making this material of high interest for photonic devices. Furthermore and rather surprising, the photografted polystyrene brushes exhibit an unusual high negative birefringence, too. This negative birefringence can be attributed to a practically complete stretching of the polymer chains throughout growth in the radical chain process. As the stretched PS brushes grafted from the pCN surfaces also provide unusual surface properties, the overall system can be of great interest for photonics, but also as mechanical coating and membranes for gas separation.

have been also widely studied for their anisotropic properties in electronics and nanophotonics.<sup>[5]</sup>

The present 2D covalent material, polymeric carbon nitride (pCN), is a family of layered semiconductors with ideal formula  $C_3N_4$ , with heptazine (alternatively tri-s-triazine) units cross-linked and stacked in a graphitic-like fashion.<sup>[6,7]</sup> pCN meanwhile found many uses, also in polymer science,<sup>[8,9]</sup> but recently attracted most attention as a photocatalyst active under visible light irradiation.<sup>[4,7,10]</sup> Due to its graphitic structure, pCN is expected to show a significant anisotropy.<sup>[11]</sup> However, only few studies are reported on anisotropic properties of pCN materials. One of the few examples was recently reported by Noda et al. who reported on the anisotropic in-plane and out-of-plane electrical

conductivity, with about two orders of magnitude higher conductivity between the layers than along the plane.<sup>[12]</sup> In another study, Arazoe et al. investigated the pCN actuation in response to humidity variation revealing an anisotropic swelling of the pCN structure.<sup>[13]</sup> Very recently, our group reported on the synthesis and high refractive index properties of homogeneous pCN thin films with optical quality by chemical vapor deposition (CVD).<sup>[14]</sup> The as-prepared films show an extremely high refractive index ( $n_D = 2.43$ ), which is even in the range of diamond. In a further study, the photoactivity of so-formed pCN thin films were used to initiate a radical photopolymerization to form polymer brushes of some benchmark vinyl monomers, such as poly-dimethylacrylamide, -allylamine, -*N*-vinylimidazole, -*N*-isopropylacrylamide, -methyl methacrylate, and -styrene, covalently on the pCN surface, and the resulting very thick polymer brushes were attributed to a directional and clean growth of the brushes normal to the pCN surface.<sup>[9]</sup> Herein, we extend these two papers by analyzing the anisotropy of pCN optical functions and the material properties of the very unusual polystyrene (PS) brushes photografted from pCN surface.

Optical anisotropy is a fundamental property for light manipulation due to birefringence that causes the incoming light beam to split into two different rays, namely ordinary and extraordinary ray, in uniaxial optical materials.<sup>[15]</sup> The performance of optical components based on anisotropic materials depend on the birefringence ( $\Delta n$ ) of the constituting materials. Large  $\Delta n$  enable smaller and more efficient devices.<sup>[15]</sup> Transition metal dichalcogenides recently received a lot of attention due to their giant birefringence  $\approx 1.5$  in the IR, where no optical absorption occurs. However, only few materials with high

## 1. Introduction

Anisotropy is commonly referred to as the condition of having different property values along different directions. In materials, it is related to their structure, and it affects the electrical, magnetic, optical, and mechanical response to an external stimulus.<sup>[1]</sup> 2D covalent layered materials usually possess record-high direction-dependent properties due to their intra-layer covalent bonding and inter-layer van der Waals interactions.<sup>[2–4]</sup> Recently, transition metal dichalcogenides, such as  $MoS_2$ , already delivered excellent performances in logic and optoelectronic devices, such as field effect transistors and photodetectors.<sup>[2]</sup> Graphene and hexagonal boron nitride (h-BN)

P. Giusto, B. Kumru, M. Antonietti  
Max Planck Institute of Colloids and Interfaces  
Department of Colloid Chemistry  
Am Mühlenberg 1, 14476 Potsdam, Germany  
E-mail: paolo.giusto@mpikg.mpg.de; Baris.Kumru@mpikg.mpg.de

D. Cruz  
Department of Inorganic Chemistry  
Fritz-Haber-Institut der Max-Planck-Gesellschaft  
Faradayweg 4–6, 14195 Berlin, Germany

 The ORCID identification number(s) for the author(s) of this article can be found under <https://doi.org/10.1002/adom.202101965>.

© 2021 The Authors. Advanced Optical Materials published by Wiley-VCH GmbH. This is an open access article under the terms of the Creative Commons Attribution License, which permits use, distribution and reproduction in any medium, provided the original work is properly cited.

DOI: 10.1002/adom.202101965

birefringence and high transparency in the visible range were reported so far. h-BN exhibits a strong negative birefringence, i.e., higher out-of-plane refractive index, while possessing a large bandgap ( $\approx 6$  eV).<sup>[16]</sup> Inspired by these results, we can expect high birefringence occurring also in the analogous 2D covalent materials, such as carbon nitrides, boron carbon nitrides, and more.<sup>[17]</sup> Therefore, we investigate the optical anisotropy of pCN thin films by ellipsometry. Using this occasion, we also analyze the optical anisotropy of the PS brushes photografted from the pCN surface which were already expected to reveal practically perfect directional growth normal to the pCN surface, thus providing us with further insights into the polymer chemistry of brush growth mechanism.<sup>[9]</sup> Optical anisotropy in linear polymers, birefringence values, and sign depends on the orientation of the transition dipole moment with respect to the chain axis. When the transition dipole moment is almost perpendicular to the chain direction, negative birefringence occurs.<sup>[18,19]</sup> In other linear polymer semiconductors, such as polyphenylenes and polythiophenes, the degree of anisotropy could be correlated to an increased regioregularity and crystallinity in the polymer films.<sup>[18,20]</sup> Therefore, birefringence studies can provide further information on the polymer local structure and thus is a powerful technique for material chemists especially concerning thin film materials.<sup>[18]</sup>

## 2. Results and Discussion

pCN is constituted by heptazine units, covalently cross-linked by nitrogen bridges in a 2D network, and stacked in a graphitic fashion with interlayer distance of 0.32 nm (Figure 1a).<sup>[14]</sup> While the very high refractive index of pCN thin films with high

transparency, high homogeneity, and low roughness ( $\approx 1$  nm, Figure S1, Supporting Information) in the visible range using an isotropic model was already reported,<sup>[14]</sup> we use here measurement and data evaluation techniques to determine the expected optical anisotropy. The experimental data expressed as extinction coefficient ( $k$ ), ordinary and extraordinary refractive indices ( $n_o$  and  $n_{eo}$ ), birefringence ( $\Delta n$ ) versus wavelength are shown in Figure 1b,c. Indeed, the pCN thin film shows a strong birefringence in the visible range with a very high ordinary refractive index ( $n_{o,D}$ ) of 2.54, which accounts for the in-plane (a, b plane) refractive index, while the extraordinary refractive index ( $n_{eo,D}$ ) of 1.83 is comparably low. The calculated birefringence  $\Delta n_D$  of 0.71 ( $n_{o,D} - n_{eo,D}$ ), i.e. the difference between the in-plane and out-of-plane refractive indices, is indeed very high making the pCN thin films a very good candidate for photonic and optoelectronic devices exploiting large optical anisotropy such as photodetectors, quantum computers, visible light communication, polarizers, microphotonic polarization converters, and many others.<sup>[15,16,21]</sup> Ideal diamond does not present anisotropy due to its well-defined isotropic cubic lattice structure. Diamond birefringence was detected only in stress- or strain-induced diamond (or inclusions of impurities) which causes distortion of the cubic lattice.<sup>[22]</sup> As expected, the optical birefringence of pCN increases close to the bandgap (2.88 eV, 431 nm) and decreases towards the NIR with  $\Delta n_{1000\text{ nm}}$  of 0.66 (Figure 1c), due to the increased oscillators strength closer to the bandgap. Furthermore, the strong birefringence in pCN thin films speaks for a high degree of order achieved in the material, in good agreement with our previous report. Such giant birefringence in layered graphitic-like materials was recently reported for h-BN with similar values to pCN in the visible range, but negative, i.e. possessing higher out-plane refractive

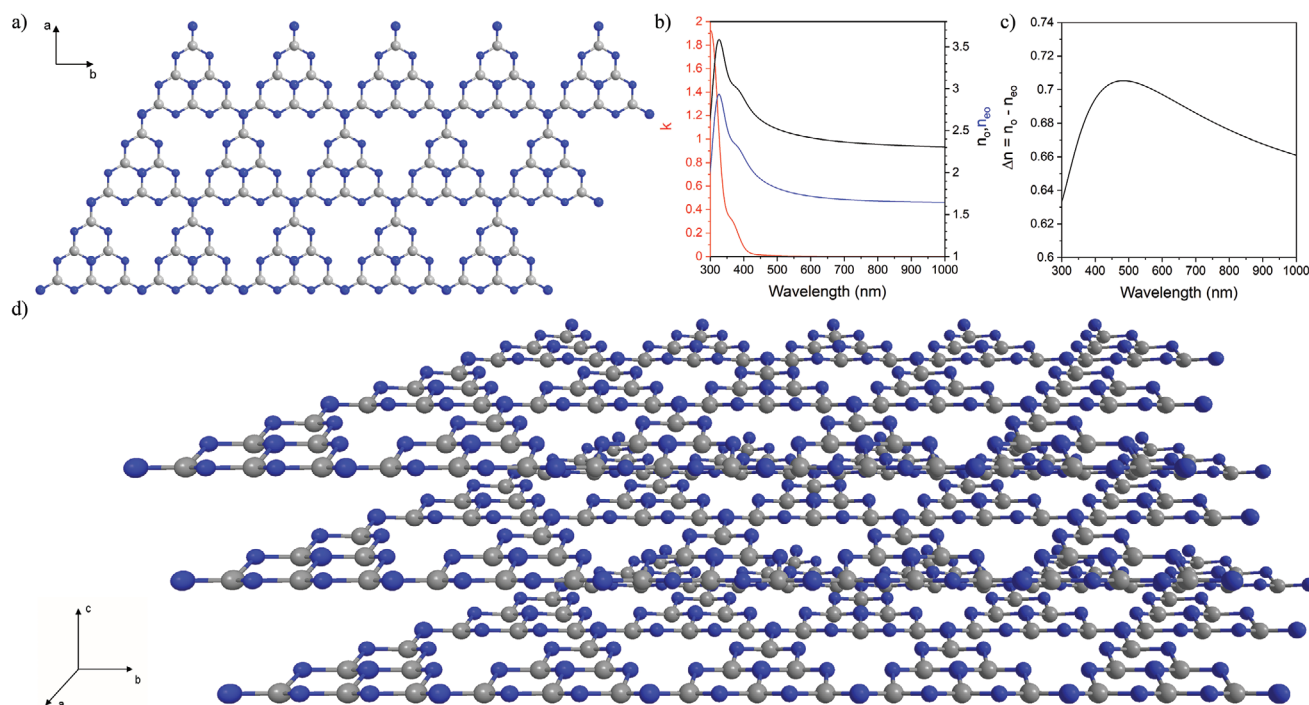


**Figure 1.** a) Chemical structure of pCN layer, blue balls are representing nitrogen atoms, dark gray corresponds to carbon atoms; b) stacked structure of pCN;<sup>[24]</sup> c) optical properties of pCN; d) birefringence of pCN as a function of wavelength.

index and a lower in-plane one.<sup>[16]</sup> The pCN thin films did not show any dichroism, however, an anisotropic behavior is found for imaginary part of the dielectric function ( $\epsilon_2$ ), i.e. real and imaginary permittivity between along a,b- versus the c-plane are different (Figure S2, Supporting Information). Interestingly, the fitting of the ellipsometric data reveals that the pCN layers are about perfectly stacked on top of each other, but with a tilt angle: the Euler angle theta ( $\theta$ ), that describe the relative tilting with respect to the vertical axis, reveal that the units are shifted with respect to the normal by about  $-25^\circ(+180^\circ > \theta > -180^\circ)$ .<sup>[23]</sup> These results suggest the presence of a graphitic structure, where the pCN layers grow in a rhombohedral structure tilted with respect to the vertical axis (Figure 1d). This corresponds to a relative shift of 0.084 nm from one layer to the next or 2/3 of a single C–N bond, i.e. the shift is rather typical for graphitic materials, but adds up in an A-A-A layer fashion. This was not described for carbon nitride structures before and will improve the understanding of carbon nitride behavior as such.

We then used this more complete model of optical properties to characterize also polystyrene layers grafted on top of the carbon nitride thin film. With such layers of adjustable thickness, light inclusion can be optimized. Photoinitiation from pCN yields exclusively covalently bound pCN-polymer chains unless radical transfer agents are employed.<sup>[9,25]</sup> Therefore, shining light directly on a carbon nitride thin film surface coated with a styrene monomer enables the covalent growth of PS brushes at the pCN surface. We already proposed a “skyscraper-like” vertical growth mechanism of the brushes due to space constraints, based on secondary properties, but could not prove that before. Therefore, we investigated also the PS photografted from pCN surfaces, making the ellipsometric characterization also useful for structural characterization of polymer brushes. Linear atactic polymers such as PS are usually arranged in the so-called thermodynamically more favorable “random coil,” which allows minimizing the conformation entropy and providing isotropic properties to the material. As shown in Figure 2a, the as-grown PS brushes photografted from the carbon nitride binding layer reveal negative birefringence in the visible range with  $\Delta n_D$  of  $-0.18/-0.19$  for brushes of 28 (2 h polymerization time) and 96 nm (4 h polymerization time) respectively, that is rather independent to the film thickness. This further supports our previous assumption on the brushes being highly strained, where the PS brushes have to grow in a close to perfect stretched conformation due to geometrical constraints. In this arrangement, the main transition dipole moment from the phenyl group is almost perpendicular to the main alkyl chain.

Uniaxial strain can induce various degrees of optical birefringence in PS as previously reported.<sup>[26,27]</sup> PS indeed possesses in general negative birefringence which is attributed to the phenyl groups orientation with respect to the main chain.<sup>[27,28]</sup> A value of birefringence of  $-0.2$  was however only reported for syndiotactic polystyrene, in which the polymer chains are indeed perfectly aligned (except in surface defects). Interestingly we found that in our brushes, the orientation is as high as in the syndiotactic state. A further proof for a growth rather by organized packing than transport properties is given by the optical Euler angles. Indeed,  $\theta$  shows a value of  $126^\circ$  for the PS brushes, indicating a significant deviation from vertical growth with respect to the pCN film. This is also about the unit cell angle of  $\delta$  form of syndiotactic polystyrene (monoclinic,  $121.2^\circ$ ), i.e. it looks that PS brushes grow epitaxially onto the flat and uniform carbon nitride binder.<sup>[29]</sup>

Removing PS grafted pCN thin film from the substrate is a high effort due to strong covalent binding to the carbon nitride binder layer, however a small piece was removed by crashing the sample in order to investigate it under the optical microscope (Figure 3a). Anisotropic cracks are typical for PS samples, and applying polarization on this area confirms the strong birefringence, especially located on the cracks (PS). Such a facile imaging enhances the conclusion towards oriented PS on pCN thin films. Furthermore, similar measurement was performed by angular tilting of the incoming light source (Figure 3b). Evolution of the optical response by the function of the angle of the incoming light is depicted in Figure 3b. We attribute the black particles to a silicon substrate and the edge as a pCN thin film and the changes in the main body (PS) are clearly visible. Additionally, FT-IR spectra of peeled pCN thin film and PS photografted peeled pCN thin films are represented in Figure S3 (Supporting Information), which elucidates a change in the spectra after PS photografting.

### 3. Conclusion

Ellipsometry was employed to characterize the properties of pCN thin films and photografted-from PS brushes. On the one hand, the results reveal a very high birefringence for pCN thin films with in-plane  $n_D = 2.54$  and high birefringence ( $\Delta n_D$ ) of 0.71, which makes the pCN thin films a very good candidate for photonic and optoelectronic devices exploiting large optical anisotropy such as photodetectors, quantum computers, communication, polarizers, microphotonic polarization converters, and further.<sup>[15,16,21]</sup> On the other hand, the composite which confirmed a vertical growth of polymer chains as well as

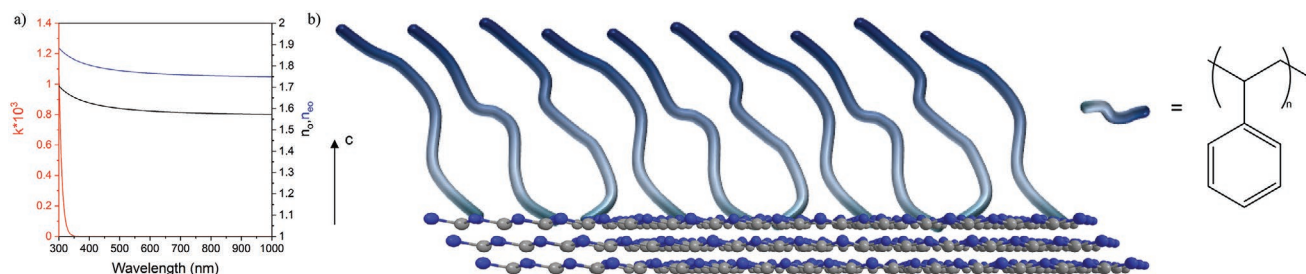


**Figure 2.** a) Anisotropic optical properties of photografted PS brushes; b) schematic representation of the grown brushes on the pCN surface.

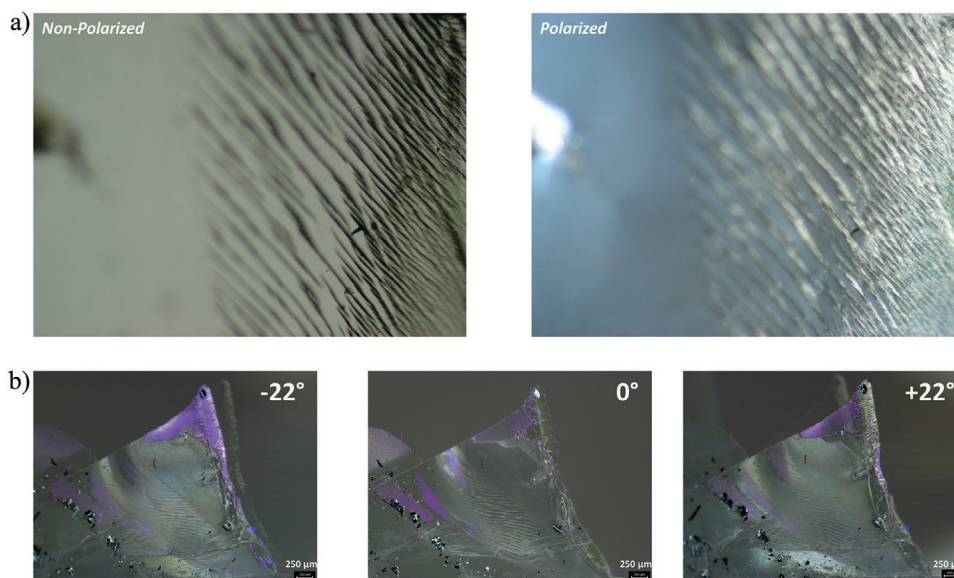


**Figure 3.** a) Non-polarized and polarized top-down optical images of photografted PS brushes on pCN thin film, b) angular tilted polarized optical images of photografted PS brushes on pCN thin film.

a negative birefringence by means of optical anisotropy. From the optical perspective, such bilayer structure possessing positive and negative birefringence is of particular interest as retardation film. Retardation films are widely used as polarization transformation materials especially for flat panel displays. Furthermore, we expect that this technology can find application also in high performing mechanical coatings and gas separation membranes.

#### 4. Experimental Section

All materials were used as purchased, melamine (99%, Sigma Aldrich), styrene (99%, Sigma Aldrich), tetrahydrofuran (THF, 99%, Sigma Aldrich). 50 W LED chips (420 nm visible light) were connected to a self-made circuit and cooling system.

**Experimental Part: Synthesis of pCN Thin Films:** The preparation of pCN thin films was conducted in a two-zone CVD reactor (planarGROW-3S-OS CVD System from planarTECH), as previously reported.<sup>[14]</sup> In typical recipe, 7–10 g of melamine were placed in a glass holder and heated up at 300 °C (10° per minute) in vacuum (10 Torr), using silicon with grown silicon dioxide (nominal value 100 nm) as substrates, provided by Microchemicals. The substrates for the deposition were placed in the second zone and heated up at 550 °C for 90 min. The samples were left to cool down naturally at room temperature and collected after breaking the chamber vacuum.

**Synthesis of Polystyrene-Grafted pCN Thin Films:** The pCN thin film surfaces were covered with styrene (0.5 ml) and irradiated via visible light for 2 and 4 h as reported previously. After the illumination, surfaces were washed with THF to remove excess of monomers and unbound polymers. The films were further dried at room temperature before conducting measurements.

**Characterization:** Ellipsometric measurements were performed using Woollam M-2000 ellipsometer in the range 300–1000 nm at 65–70–75° by generalized ellipsometry. The data have been fitted using CompleteEASE software provided by Woollam. For pCN thin films, the oscillators, and optical functions reported in ref. [14] were used and for photografted PS layers the software's optical functions have been used in an anisotropic model. The reported optical functions were obtained as best fit among 2–4 samples measured in 2–3 different points each. Optical microscopy images of peeled pCN-PS were collected via DM1000 Leica. Angular

optical microscopy measurements were performed on Leica DVM6 Digital microscope.

#### Supporting Information

Supporting Information is available from the Wiley Online Library or from the author.

#### Acknowledgements

P.G. and B.K. contributed equally to this work. The authors thank Max Planck Society for funding. They are grateful for Bolortuya Badamdorj for the light microscopy measurements and Marlies Gräwert for SEC measurement and Francesco Brandi for general help and discussion. The authors thank prof. Maddalena Patrini and Dr. Giovanni Manfredi for the help with data interpretation and fruitful discussion.

Open access funding enabled and organized by Projekt DEAL.

#### Conflict of Interest

The authors declare no conflict of interest.

#### Data Availability Statement

The data that support the findings of this study are available from the corresponding author upon reasonable request.

#### Keywords

birefringence, carbon nitride, polymer brushes, refractive index, thin films

Received: September 14, 2021

Revised: November 10, 2021

Published online: December 18, 2021

- [1] L. Vannucci, U. Petralanda, A. Rasmussen, T. Olsen, K. S. Thygesen, *J. Appl. Phys.* **2020**, *128*, 105101.
- [2] S. Zhao, B. Dong, H. Wang, H. Wang, Y. Zhang, Z. V. Han, H. Zhang, *Nanoscale Adv.* **2020**, *2*, 109.
- [3] M. Liu, Y. Ishida, Y. Ebina, T. Sasaki, T. Hikima, M. Takata, T. Aida, *Nature* **2015**, *517*, 68.
- [4] K. Sakaushi, M. Antonietti, *Acc. Chem. Res.* **2015**, *48*, 1591.
- [5] a) F. Xia, H. Wang, D. Xiao, M. Dubey, A. Ramasubramaniam, *Nat. Photonics* **2014**, *8*, 899; b) C. Wang, G. Zhang, S. Huang, Y. Xie, H. Yan, *Adv. Opt. Mater.* **2020**, *8*, 1900996.
- [6] C. Jia, L. Yang, Y. Zhang, X. Zhang, K. Xiao, J. Xu, J. Liu, *ACS Appl. Mater. Interfaces* **2020**, *12*, 53571.
- [7] S. Mazzanti, G. Manfredi, A. J. Barker, M. Antonietti, A. Savateev, P. Giusto, *ACS Catal.* **2021**, *11*, 11109.
- [8] a) Q. Cao, B. Kumru, M. Antonietti, B. V. Schmidt, *Macromolecules* **2019**, *52*, 4989; b) B. Kumru, D. Cruz, T. Heil, B. V. Schmidt, M. Antonietti, *J. Am. Chem. Soc.* **2018**, *140*, 17532; c) B. Kumru, M. Shalom, M. Antonietti, B. V. Schmidt, *Macromolecules* **2017**, *50*, 1862.
- [9] P. Giusto, B. Kumru, J. Zhang, R. Rothe, M. Antonietti, *Chem. Mater.* **2020**, *32*, 7284.
- [10] a) B. Kumru, M. Antonietti, *Adv. Colloid Interface Sci.* **2020**, 102229; b) S. Mazzanti, A. Savateev, *ChemPlusChem* **2020**, *85*, 2499; c) I. Ghosh, J. Khamrai, A. Savateev, N. Shlapakov, M. Antonietti, B. König, *Science* **2019**, *365*, 1801; d) Z. Gan, Y. Shan, J. Chen, Q. Gui, Q. Zhang, S. Nie, X. Wu, *Nano Res.* **2016**, *9*, 1801.
- [11] J. Liu, H. Wang, Z. P. Chen, H. Moehwald, S. Fiechter, R. van de Krol, L. Wen, L. Jiang, M. Antonietti, *Adv. Mater.* **2015**, *27*, 712.
- [12] Y. Noda, C. Merschjann, J. Tarábek, P. Amsalem, N. Koch, M. J. Bojdys, *Angew. Chem.* **2019**, *131*, 9494.
- [13] H. Arazoe, D. Miyajima, K. Akaike, F. Araoka, E. Sato, T. Hikima, M. Kawamoto, T. Aida, *Nat. Mater.* **2016**, *15*, 1084.
- [14] P. Giusto, D. Cruz, T. Heil, H. Arazoe, P. Lova, T. Aida, D. Comoretto, M. Patrini, M. Antonietti, *Adv. Mater.* **2020**, *32*, 1908140.
- [15] G. Ermolaev, D. Grudin, Y. Stebunov, K. Voronin, V. Kravets, J. Duan, A. Mazitov, G. Tselikov, A. Bylinkin, D. Yakubovsky, *Nat. Commun.* **2021**, *12*, 854.
- [16] A. Segura, L. Artús, R. Cuscó, T. Taniguchi, G. Cassabo, B. Gil, *Phys. Rev. Mater.* **2018**, *2*, 024001.
- [17] a) S. Cao, J. Low, J. Yu, M. Jaroniec, *Adv. Mater.* **2015**, *27*, 2150; b) N. Fechner, N. P. Zussblatt, R. Rothe, R. Schlögl, M. G. Willinger, B. F. Chmelka, M. Antonietti, *Adv. Mater.* **2016**, *28*, 1287; c) K. Sakaushi, H. Nishihara, *Acc. Chem. Res.* **2021**, *54*, 3003; d) P. Giusto, D. Cruz, T. Heil, N. Tarakina, M. Patrini, M. Antonietti, *Adv. Sci.* **2021**, *8*, 2101602; e) P. Giusto, H. Arazoe, D. Cruz, P. Lova, T. Heil, T. Aida, M. Antonietti, *J. Am. Chem. Soc.* **2020**, *142*, 20883.
- [18] M. Campoy-Quiles, M. I. Alonso, D. D. Bradley, L. J. Richter, *Adv. Funct. Mater.* **2014**, *24*, 2116.
- [19] M. Campoy-Quiles, J. Nelson, P. Etchegoin, D. Bradley, V. Zhokhavets, G. Gobsch, H. Vaughan, A. Monkman, O. Ingänes, N.-K. Persson, *Phys. Status Solidi C* **2008**, *5*, 1270.
- [20] M. Galli, F. Marabelli, D. Comoretto, *Appl. Phys. Lett.* **2005**, *86*, 201119.
- [21] a) C. H. Lin, C. Y. Kang, T. Z. Wu, C. L. Tsai, C. W. Sher, X. Guan, P. T. Lee, T. Wu, C. H. Ho, H. C. Kuo, *Adv. Funct. Mater.* **2020**, *30*, 1909275; b) J. Liu, H. Wang, M. Antonietti, *Chem. Soc. Rev.* **2016**, *45*, 2308.
- [22] D. Howell, *Eur. J. Mineral.* **2012**, *24*, 575.
- [23] D. Schmidt, B. Booso, T. Hofmann, E. Schubert, A. Sarangan, M. Schubert, *Appl. Phys. Lett.* **2009**, *94*, 011914.
- [24] In Figure 1a and 1b we reported the ideal structure of carbon nitride (C<sub>3</sub>N<sub>4</sub>) to clarify what is the relation between our findings and the chemical structure.
- [25] N. Yandrapalli, T. Robinson, M. Antonietti, B. Kumru, *Small* **2020**, *16*, 2001180.
- [26] A. Uchiyama, T. Yatabe, *Jpn. J. Appl. Phys.* **2003**, *42*, 3503.
- [27] A. Uchiyama, Y. Ono, Y. Ikeda, H. Shuto, K. Yahata, *Polym. J.* **2012**, *44*, 995.
- [28] P. Rizzo, A. R. Albulnia, G. Guerra, *Macromol. Chem. Phys.* **2009**, *210*, 2148.
- [29] E. B. Gowd, K. Tashiro, C. Ramesh, *Prog. Polym. Sci.* **2009**, *34*, 280.